Published in final edited form as:
Cancer Res. 2014 March 15; 74(6): 1651–1660. doi:10.1158/0008-5472.CAN-13-3159.

PCAT-1, a long noncoding RNA, regulates BRCA2 and controls homologous recombination in cancer

John R. Prensner[1,2,14], **Wei Chen**[3,14], **Matthew K. Iyer**[1], **Qi Cao**[1,2], **Teng Ma**[4], **Sumin Han**[3], **Anirban Sahu**[1], **Rohit Malik**[1], **Kari Wilder-Romans**[3], **Nora Navone**[5], **Christopher J. Logothetis**[5], **John C. Araujo**[5], **Louis L. Pisters**[5], **Ashutosh K. Tewari**[6], **Christine E. Canman**[7], **Karen E. Knudsen**[8], **Naoki Kitabayashi**[9], **Mark A. Rubin**[9], **Francesca Demichelis**[9,10], **Theodore S. Lawrence**[3], **Arul M. Chinnaiyan**[1,2,11,12,13,15], and **Felix Y. Feng**[1,3,12,15]

[1]Michigan Center for Translational Pathology, University of Michigan Medical School, Ann Arbor, Michigan, USA 48109

[2]Department of Pathology, University of Michigan Medical School, Ann Arbor, Michigan, USA 48109

[3]Department of Radiation Oncology, University of Michigan Medical School, Ann Arbor, Michigan, USA 48109

[4]Department of Internal Medicine, University of Michigan Medical School, Ann Arbor, Michigan, USA 48109

[5]Department of Genitourinary Medical Oncology, M.D. Anderson Cancer Center, Houston, TX, USA 77030

Address correspondence to: Felix Y Feng, M.D., Department of Radiation Oncology, University of Michigan Medical Center, 1500 E Medical Center Drive, UHB2C490-SPC5010, Ann Arbor, MI 48109-5010, Phone: 734-936-4302; Fax: 734-763-7371, ffeng@med.umich.edu. Arul M. Chinnaiyan, M.D. Ph.D., Comprehensive Cancer Center, University of Michigan Medical School, 1400 E. Medical Center Dr., 5316 CCGC 5940, Ann Arbor, MI 48109-5940, Phone: 734-615-4062; Fax: 734-615-4055, arul@med.umich.edu.

[14]These authors contributed equally

[15]These authors share senior authorship

Author Contributions

Conception and design: J.R. Prensner, W. Chen, A.M. Chinnaiyan, F.Y. Feng

Development of methodology: W. Chen, J.R. Prensner, S. Han, T. Ma, M.K. Iyer, F.Y. Feng

Acquisition of data: W. Chen, J.R. Prensner, Q. Cao, T. Ma, R. Malik, A. Sahu, S. Han, K. Wilder-Romans, C.E. Canman, N. Navone, C.J. Logothetis, J.C. Araujo, L.L. Pisters, A.K. Tewari, N. Kitabayashi, M.A. Rubin, F. Demichelis, F.Y. Feng

Analysis and interpretation of data: M.K. Iyer, W. Chen, J.R. Prensner, F.Y. Feng

Writing, review and/or revision of the manuscript: J.R. Prensner, W. Chen, M.K. Iyer, A.M. Chinnaiyan, F.Y. Feng

Administrative, technical, or material support: T.S. Lawrence, K.E. Knudsen, F.Y. Feng

Study supervision: J.R. Prensner, A.M. Chinnaiyan, F.Y. Feng

Conflicts of Interest

The University of Michigan has filed a patent on PCAT1 in which A.M.C., J.R.P. and M.K.I. are named as co-inventors. Wafergen, Inc. has a non-exclusive license for creating commercial research assays for the detection of lncRNAs including PCAT1. A.M.C. serves on the Scientific Advisory Board of Wafergen. Wafergen had no role in the design or experimentation of this study, nor has it participated in the writing of the manuscript. A.K.T. is a co-inventor on a patent regarding a prostatectomy method for diagnosing and staging prostate cancer. A.K.T. also has received sponsored funding and/or honoraria from Intuitive Surgical, Boston Scientific, and Medtronics, none of whom were involved in the writing of this manuscript.

[6]Department of Urology, Institute of Prostate Cancer and LeFrak Center For Robotic Surgery, Weill Cornell Medical College and New York Presbyterian Hospitals, New York, New York, USA 10065

[7]Department of Pharmacology, University of Michigan Medical School, Ann Arbor, Michigan, USA 48109

[8]Departments of Cancer Biology, Urology, and Radiation Oncology, Thomas Jefferson University, Philadelphia, Pennsylvania USA 19107

[9]Department of Pathology and Laboratory Medicine, Weill Cornell Medical College, New York, New York, USA 10065

[10]Centre for Integrative Biology, University of Trento, Trento, Italy 38122

[11]Department of Urology, University of Michigan Medical School, Ann Arbor, Michigan, USA 48109

[12]Comprehensive Cancer Center, University of Michigan Medical School, Ann Arbor, Michigan, USA 48109

[13]Howard Hughes Medical Institute, University of Michigan Medical School, Ann Arbor, Michigan, USA 48109

Abstract

Impairment of double-stranded DNA break (DSB) repair is essential to many cancers. However, while mutations in DSB repair proteins are common in hereditary cancers, mechanisms of impaired DSB repair in sporadic cancers remain incompletely understood. Here, we describe the first role for a long noncoding RNA (lncRNA) in DSB repair in prostate cancer. We identify *PCAT-1*, a prostate cancer outlier lncRNA, which regulates cell response to genotoxic stress. *PCAT-1* expression produces a functional deficiency in homologous recombination (HR) through its repression of the *BRCA2* tumor suppressor, which, in turn, imparts a high sensitivity to small molecule inhibitors of *PARP1*. These effects reflected a post-transcriptional repression of the *BRCA2* 3′UTR by *PCAT-1*. Our observations thus offer a novel mechanism of “BRCA-ness” in sporadic cancers.

Keywords

prostate cancer; long noncoding RNA; homologous recombination

INTRODUCTION

The uncontrolled accumulation of double-stranded DNA breaks (DSBs) represents a putative Achilles heel for cancer cells, since these lesions are toxic and their repair requires re-ligation of disrupted genetic material (1–3). Several mechanisms, such as non-homologous end joining (NHEJ), microhomology-mediated end joining (MMEJ) and homologous recombination (HR), contribute to DSB repair and are employed variously during cell cycle depending on whether a specific DSB harbors either large, small, or no stretches (NHEJ, MMEJ, and HR, respectively) of complementary DNA sequences on the

two fragments of broken DNA (4). In particular, the lethality of excess DSBs has been exploited for the therapeutic treatment of hereditary breast and ovarian cancers harboring *BRCA1/2* mutations, which leads to defective HR and increased DSBs (5). These cancers exhibit synthetic lethality when treated with small molecule inhibitors of the *PARP1* DNA repair enzyme, whose inhibition prevents a second method of DNA repair and leads to gross collapse of cellular DNA maintenance (6–8).

Recently, long noncoding RNAs (lncRNAs) have emerged as new layer of cell biology (9), contributing to diverse biological processes. In cancer, aberrant expression of lncRNAs is associated with cancer progression (9, 10), and overexpression of oncogenic lncRNAs can promote tumor cell proliferation and metastasis through transcriptional regulation of target genes (11–13). Recent studies have also identified lncRNAs induced by genotoxic stress as well as involved in the repair of DNA damage (14, 15); however, the role of lncRNAs in the regulation of DSB repair remains unclear.

Here, we report the characterization of *PCAT-1* as a prostate cancer lncRNA implicated in the regulation of DSB repair. We find that *PCAT-1* represses the BRCA2 tumor suppressor gene, leading to downstream impairment of HR. Importantly, *PCAT-1* expressing cells exhibit a BRCA-like phenotype, resulting in cell sensitization to PARP1 inhibitors. In human prostate cancer tissues, high *PCAT-1* expression predicts for low *BRCA2* expression, supporting our observations in model systems. To our knowledge, this report is the first to demonstrate a role for lncRNAs in the regulation of DSBs in prostate cancer and suggests a new mechanistic basis for impaired HR in this disease.

MATERIALS AND METHODS

For full details on methodology, please refer to the Supplementary Information for a complete Materials and Methods section.

Patient samples

For the University of Michigan patient samples, prostate tissues were obtained from the radical prostatectomy series and Rapid Autopsy Program at the University of Michigan tissue core. These programs are part of the University of Michigan Prostate Cancer Specialized Program Of Research Excellence (S.P.O.R.E.). All tissue samples were collected with informed consent under an Institutional Review Board (IRB) approved protocol at the University of Michigan. (SPORE in Prostate Cancer (Tissue/Serum/Urine) Bank Institutional Review Board # 1994-0481). For the Weill Cornell Medical College patient samples, prostate tissues were collected as part of an IRB approved protocol at Weill Cornell Medical College.

Cell lines

All cell lines were obtained from the American Type Culture Collection (Manassas, VA). Cell lines were maintained using standard media and conditions. Du145-derived cell lines were maintained in DMEM supplemented with 10% FBS (Invitrogen) and 1% penicillin-streptomycin (Invitrogen) in a 5% CO_2 cell culture incubator. RWPE-derived cell lines were maintained in KSF (Invitrogen) supplemented with Bovine Pituitary Extract, Epidermal

Growth Factor and 1% penicillin-streptomycin in a 5% CO_2 cell culture incubator. LNCAP-derived and PC3-derived were maintained in RPMI 1640 (Invitrogen) supplemented with 10% FBS and 1% penicillin-streptomycin in a 5% CO_2 cell culture incubator.

PC3 cells containing the GFP HR assay construct were generated as described previously (16, 17).

PCAT-1 or control-expressing cell lines were generated by cloning *PCAT-1* or control *LacZ* into the pLenti6 vector (Invitrogen). After confirmation of the insert sequence, lentiviruses were generated at the University of Michigan Vector Core and transfected into RWPE or Du145 cells. Stably-transfected cells were selected using blasticidin (Invitrogen).

For LNCAP cells with stable knockdown of *PCAT-1*, cells were seeded at 50–60% confluency, incubated overnight, and transfected with *PCAT-1* or non-targeting shRNA lentiviral constructs for 48 hours. GFP+ cells were drug-selected using 1 ug/mL puromycin. *PCAT-1* shRNAs were customed generated by Systems Biosciences using the following sequences: shRNA 1 GCAGAAACACCAAUGGAUAUU; shRNA 2 AUACAUAAGACCAUGGAAAU.

To ensure cell identity, all cell lines were used for fewer than 6 months after resuscitation and confirmed by genotyping after resuscitation. DNA samples were diluted to 0.10ng/ul and nine genotyping loci (D3S1358, D5S818, D7S820, D8S1179, D13S317, D18S51, D21S11, FGA, vWA and the Amelogenin locus) were analyzed by the University of Michigan DNA Sequencing Core using the Profiler Plus PCR Amplification Kit (Applied Biosystems, Foster City, CA).

Cell line assays

LNCaP, Du145, PC3, and RWPE cell lines were obtained from the American Type Culture Collection (ATCC) and maintained in standard conditions. Stable overexpression and knockdown cell lines were generated with lentiviral constructs with blasticidin or puromycin selection as appropriate. RNA isolation and cDNA synthesis were performed according to standard protocols. Quantitative PCR was performed with Power SYBR Green Mastermix on an Applied Biosystems 7900HT Real-Time PCR system. Chemosensitivity assays were performed on 5000 cells plated per well in 96 well plates and treated with a single dose of Olaparib or ABT-888 as indicated for 72 hours. WST assays (Roche) were performed according to the manufacturer's instructions. Immunofluorescence experiments were performed with 1 x 10^5 cells in 12-well plates according to standard protocols; RAD51 and γ-H2AX staining was performed 6 hours or 24 hours post-treatment, respectively.

Luciferase Assays

The indicated cell lines were transfected with full length *BRCA2* luciferase constructs as well as pRL-TK vector as internal control for luciferase activity. Following 2 days of incubation, the cells were lysed and luciferase assays conducted using the dual luciferase assay system (Promega, Madison, WI, USA). Each experiment was performed in quadruplicate.

Immunoblot Analysis

Cells were lysed in RIPA lysis buffer (Sigma, St. Louis, MO) and briefly sonicated for homogenization. Aliquots of each protein extract were boiled in sample buffer, size fractionated by SDS-PAGE at 4C, and transferred onto Polyvinylidene Difluoride membrane (GE Healthcare, Piscataway, NJ). The membrane was then incubated at room temperature for 1–2 hours in blocking buffer [Tris-buffered saline, 0.1% Tween (TBS-T), 5% nonfat dry milk] and incubated at 4C with the appropriate antibody. Following incubation, the blot was washed 4 times with TBS-T and incubated with horseradish peroxidase-conjugated secondary antibody. The blot was then washed 4 times with TBS-T and twice with TBS, and the signals visualized by enhanced chemiluminescence system as described by the manufacturer (GE Healthcare).

The following antibodies were used for immunoblot analysis: BRCA2 (EMD OP95), BRCA1 (Cell Signaling #9025S), XRCC1 (Abcam ab1838), XRCC3 (Abcam ab97390), XRCC4 (GeneTex GTX83406), Ku70 (BD Biosciences #611892), Ku80 (Cell Signaling #2180S), γ-H2AX (Cell Signaling #9718) and B-actin (Sigma A5441).

For immunoblot densitometry, the densitometric scan of the immunoblots was performed using ImageJ. Three replicate experiments were quantified for the final analysis.

Xenograft assays

Xenograft experiments were performed according to University of Michigan-approved protocols and conform to their relevant regulatory standards. Five week-old male SCID mice (CB.17. SCID), were purchased from Charles River, Inc. (Charles River Laboratory, Wilmington, MA). 1 x 10^6 Du145-control or Du145-*PCAT-1* stable cells were resuspended in 100μl of saline with 50% Matrigel (BD Biosciences, Becton Drive, NJ) and were implanted subcutaneously into the left and right flank regions of the mice. Mice were anesthetized using a cocktail of xylazine (80–120 mg/kg, IP) and ketamine (10mg/kg, IP) for chemical restraint before tumor implantation. All tumors were staged for two weeks before starting the drug treatment. At the beginning of the third week, mice with tumors (10 tumors per treatment group, average size 150–200 mm^3) were treated with Olaparib (100mg/kg, IP twice daily five times per week) or an equal volume of DMSO control. Growth in tumor volume was recorded weekly by using digital calipers.

I-SceI Homologous Recombination Assay

We followed previously described protocols (16). Briefly, PC-3 cells with a single copy of DR-GFP were transfected with empty vector control or *PCAT-1*. *PCAT-1* transfected cells were infected with adenovirus-encoded I-SceI (adeno-I-SceI) at an MOI of 1000. Cells were harvested 3 days after infection and subjected to flow cytometry analysis for the GFP-positive cell population.

Statistical analyses for experimental studies

All data are presented as means ± standard deviation or S.E.M, as indicated. All experimental assays were performed in duplicate or triplicate. Statistical analyses shown in figures represent Fisher's exact tests or Student's t-tests, as indicated.

RESULTS

PCAT-1 regulates BRCA2 levels and homologous recombination

We previously reported the systematic nomination of lncRNAs associated with prostate cancer, termed Prostate Cancer Associated Transcripts (PCATs) (10). Among these, we noted that *PCAT-1* expression was a prostate cancer outlier associated with low levels of *BRCA2*. We therefore hypothesized that *PCAT-1* mediated the repression of *BRCA2*, and thus *PCAT-1* may be implicated in the dysregulation of HR upon genotoxic stress. To pursue this hypothesis, we generated a panel of three *in vitro* cell culture model systems: *PCAT-1* overexpression in Du145 prostate cancer cells (which lack endogenous expression of this lncRNA), *PCAT-1* overexpression in RWPE benign prostate cells (which lack endogenous expression of this lncRNA), and stable knockdown of *PCAT-1* in LNCaP prostate cancer cells (which harbor high endogenous levels of *PCAT-1* expression) (Fig. 1A, *left*).

Western blot analysis of these three isogenic models uniformly revealed strong downregulation of BRCA2 protein levels in RWPE and Du145 prostate cells and upregulation of BRCA2 in LNCaP sh-*PCAT-1* cells (Fig. 1A, *right*). To ensure that these observations were not restricted to cell line-based studies, we further confirmed an inverse relationship between *PCAT-1* and *BRCA2* in two independent cohorts of human prostate cancer samples. Using 58 prostate cancer tissues and 20 prostate cancer xenografts derived from human specimens, we found that increasing *PCAT-1* expression correlated with decreased *BRCA2* expression (Fig. 1B and Supplementary Fig. S1A). Together, these data suggest that *PCAT-1* expression antagonizes *BRCA2* expression.

Importantly, *BRCA2* inactivation impairs HR of DSBs and serves as a predictive biomarker for response to treatment with inhibitors of the *PARP1* DNA repair enzyme through synthetic lethality that results from joint inactivation of two DNA repair pathways (HR via *BRCA2* inactivation, and base excision repair via *PARP1* inhibition). Accordingly, treatment of our isogenic cell lines with either a PARP1 inhibitor (Olaparib or ABT-888) or radiation, resulted in modulation of RAD51 foci formation, which is a component of the HR pathway and a marker for engagement of the HR machinery (18). Specifically, *PCAT-1* overexpression decreased RAD51 foci formation post-therapy and *PCAT-1* knockdown increased RAD51 foci formation post-therapy in prostate (Fig. 1C and Supplementary Fig. S1B–D). We further used a well-characterized HR assay, in which cells employ HR to recombine an I-SceI-cut plasmid to produce GFP signaling (16), to evaluate the function of *PCAT-1* on HR directly. We found that transient overexpression of *PCAT-1* in PC3 prostate cancer cells resulted in a significant inhibition of GFP signaling following I-SceI-induced HR in addition to decreased RAD51 foci (Fig. 1D and Supplementary Fig. S2A–D). Of note, *PCAT-1* expression does not show substantial change following induction of DNA damage via radiation (Supplementary Fig. S2E).

PCAT-1 expression impairs DNA damage repair

Because *PCAT-1* impairs HR, genotoxic stress of *PCAT-1*-expressing cells should lead to an accumulation of DSBs, which can be visualized using gamma-H2AX (γH2AX) foci, a marker of double-stranded DNA breaks that have not been repaired (4). To test this, we

treated our isogenic Du145 and LNCaP cell line models with Olaparib, ABT-888, or radiation. As predicted, *PCAT-1* overexpression in Du145 led to an increase in γH2AX foci under stress conditions (Fig. 2A, B), indicating that *PCAT-1* impairs DSB repair in these cells. Similarly, LNCaP cells with *PCAT-1* knockdown displayed decreased levels of γH2AX foci (Fig. 2A, B). Immunoblot analysis of γH2AX protein abundance in these cells following genotoxic stress confirmed a downregulation of γH2AX with knockdown of *PCAT-1* and upregulation of γH2AX with overexpression of *PCAT-1* (Supplementary Fig. S3).

Finally, we also evaluated the ability for our isogenic cell lines to sustain growth in clonogenic survival assays, a gold-standard assay for cell viability following genotoxic stress, after treatment of cells with PARP1 inhibition or radiation. We found that *PCAT-1* expression led to decreased cell survival in Du145 and RWPE cells, whereas *PCAT-1* knockdown increased LNCaP cell survival, in these assays (Supplementary Fig. S4). To exclude a regulatory relationship between *PCAT-1* and other major actors in DNA damage, we performed analysis of XRCC1 (base excision repair pathway), XRCC3 (HR), XRCC4 (NHEJ), Ku70 (NHEJ), Ku80 (NHEJ), and BRCA1 (multiple pathways) in our *in vitro* models, which showed no change in protein abundance upon modulation of *PCAT-1* (Supplementary Fig. S5A). Together, these data indicate that *PCAT-1* expression may impart cell sensitivity to genotoxic stress by decreasing the HR response through downregulation of BRCA2.

PCAT-1 expression leads to increased cell death following genotoxic stress

Because *PCAT-1* expressing cells exhibit reduced HR efficiency when challenged, we investigated whether PARP1 inhibition selectively killed *PCAT-1*-expressing cells. Following treatment with two PARP1 inhibitors (Olaparib or ABT-888), we observed that knockdown of *PCAT-1* in LNCaP cells prevented cell death, whereas overexpression of *PCAT-1* in Du145 and RWPE prostate cells increased cell death in response to PARP inhibition (Fig. 3A, *left* and Supplementary Fig. S5B–D). This change in cell sensitivity to PARP1 inhibitors was striking, with a five-fold change in the IC50 for LNCaP and Du145 cells (Fig. 3A, *right* and Supplementary Fig. S6). Similar results were observed in RWPE cells overexpressing *PCAT-1* (Supplementary Fig. S7).

To ensure that these effects were dependent on BRCA2, we performed a rescue experiments by performing knockdown of *BRCA2* in LNCaP sh*PCAT-1* cells (which have increased levels of BRCA2). These experiments demonstrated a corresponding increase in the sensitivity of these cells to PARP1 inhibition in a dose-dependent manner according to the efficiency of the *BRCA2* knockdown (Fig. 3B). We further observed reduced RAD51 foci post-treatment following *BRCA2* knockdown in LNCaP sh*PCAT-1* cells as well (Supplementary Fig. S8). To exclude a role for altered cell cycle distributions in these phenotypes, we performed flow cytometry, which demonstrated no change in cell cycle in our model systems (Supplementary Fig. S9).

PCAT-1 expression leads to decreased in vivo tumor growth following PARP inhibition

To evaluate the contribution of *PCAT-1* to PARP inhibitor response *in vivo*, we generated xenografts of Du145 cells expressing either empty vector control or *PCAT-1*. We observed that Du145-*PCAT-1* cells grew significantly more rapidly in severe combined immunodeficient (SCID) mice, consistent with our previous findings that *PCAT-1* accelerates prostate cell proliferation *in vitro* (Fig. 3C) (10). Moreover, Du145-*PCAT-1* xenografts showed marked susceptibility and tumor regression following intra-peritoneal (IP) administration of Olaparib, whereas Du145-control cells showed only a subtle change in growth while the drug was administered, indicating that the background effect of Olaparib therapy—possibly due to its effects on other members of the PARP family (19)—is small (Fig. 3C). Mice in all groups of treatment maintained their body weights and showed no evidence of weight loss (Supplementary Fig. S10A).

Importantly, Du145 xenografts retained both *PCAT-1* expression and BRCA2 repression (Fig. 3D). To investigate *PCAT-1* signaling under control-treated (DMSO) and Olaparib-treated conditions, we also observed *in vivo* upregulation of *PCAT-1*-induced target genes (*TOP2A*, *E2F8*, *BIRC5*, and *KIF15*) (Supplementary Fig. S10B), defined by previous microarray profiling of LNCaP cells with *PCAT-1* siRNAs and confirmed in RWPE-*PCAT-1* overexpressing cells (Supplementary Fig. S10C) (10). These data suggest that *PCAT-1* is mechanistically linked to increased prostate cell sensitivity to PARP1 inhibitors via its repression of BRCA2 both *in vitro* and *in vivo*.

PCAT-1 does not operate via traditional lncRNA-mediated mechanisms

While many lncRNAs are noted to regulate gene transcription through epigenetic mechanisms (11, 13, 20), we did not observe evidence for this possibility with *PCAT-1*. While *PCAT-1* regulated *BRCA2* mRNA *in vitro* (Supplementary Fig. S11A), treatment of RWPE-*LacZ* and RWPE-*PCAT-1* cells with the DNA methylation inhibitor 5-azacytidine (5-aza), the histone deacetylase inhibitor TSA, or both did not reveal enhanced epigenetic regulation of *BRCA2* mRNA in *PCAT-1*-expressing cells (Supplementary Fig. S11B), although there was a baseline regulation of *BRCA2* in both cell lines when 5-aza and TSA were combined. Furthermore, bisulfite sequencing of the *BRCA2* promoter in our isogenic LNCaP and RWPE model systems demonstrated minimal CpG island methylation in all cell lines (Supplementary Fig. S11C). These results suggest that epigenetic repression of *BRCA2* is not the primary mechanism of *PCAT-1*. Moreover, lncRNAs containing Alu elements in their transcript sequence may utilize these repetitive sequences to regulate target gene mRNAs via STAU1-dependent degradation (21). Although *PCAT-1* harbors an Alu element from bps 1103 – 1402, knockdown of STAU1 in LNCaP or VCaP cells, which endogenously harbor *PCAT-1*, did not alter *BRCA2* levels (Supplementary Fig. S11D).

PCAT-1 regulates BRCA2 post-transcriptionally

To determine whether *PCAT-1* may function in a manner more analogous to microRNAs, which regulate mRNA levels post-transcriptionally (22), we generated a luciferase construct of the *BRCA2* 3′UTR, which is 902 bps in length (Fig. 4A). Surprisingly, we found that RWPE-*PCAT-1* cells, but not control RWPE-*LacZ* cells, were able to directly repress the activity of the wild-type *BRCA2* 3′UTR construct (Fig. 4A). Supporting these data, we

found that *PCAT-1* was localized to the cell cytoplasm (Supplementary Fig. S12A), and overexpression of *PCAT-1* in Du145 cells significantly reduced the stability of endogenous *BRCA2* mRNA, consistent with a post-transcriptional mechanism (Supplementary Fig. S12B, C).

To map a region of *PCAT-1* required for repression of the *BRCA2* 3′UTR, we additionally generated a series of *PCAT-1* deletion constructs and overexpressed these in RWPE cells (Fig. 4B and Supplementary Fig. S13A). We generated these constructs to establish whether the 3′ end of *PCAT-1*, which contains portions of ancestral transposase and Alu repeat elements (Fig. 4B) (10), or the 5′ end of *PCAT-1*, which consists of non-repetitive DNA sequences, was required for *BRCA2* repression. We observed that the 5′ end of *PCAT-1* was sufficient to downregulate the *BRCA2* 3′UTR luciferase signal as well as endogenous *BRCA2* transcript levels (Fig. 4B, C), and for this regulation, the first 250 bps of the *PCAT-1* gene were required. By contrast, the 3′ end of *PCAT-1* was expendable. Importantly, the 5′ end of *PCAT-1* was similarly sufficient to sensitize RWPE cells to Olaparib treatment *in vitro* (Fig. 4D). To rule out the possibility that RNA instability was responsible for the inactivity of the *PCAT-1* constructs, we performed RNA stability assays, which demonstrated equivalent rates of RNA decay between full-length *PCAT-1* and the inactive *PCAT-1* deletion constructs in RWPE cells (Supplementary Fig. S13B). Together, these results indicate that *PCAT-1* overexpression is able to directly repress the activity of the *BRCA2* 3′UTR, and that this repression required the 5′ end of *PCAT-1*.

DISCUSSION

To our knowledge, this is the first report of a lncRNA being involved in the DSB repair process in prostate cancer (Supplementary Fig. S14). These data are supported by a striking inverse correlation between *PCAT-1* and *BRCA2* expression in human prostate cancer samples. Our results expand the potential roles for lncRNAs in cancer biology and contrast strikingly with previous reports that lncRNAs operate epigenetically through chromatin modifying complexes (23, 24). Indeed, epigenetic regulation likely represents only a one of numerous mechanisms for lncRNA function (12, 21, 25, 26). Supporting this notion, we do not observe compelling evidence that *PCAT-1* functions in an epigenetic manner, but rather it may exhibit post-transcriptional regulation of its target genes.

Importantly, *PCAT-1* is also predominantly cytoplasmic, and thus our work describes the first cytoplasmic prostate lncRNA to be associated with therapeutic response. Cytoplasmic lncRNAs are also less well explored than their nuclear counterparts, and our work sheds light onto the complex mechanistic regulation of cellular processes via cytoplasmic lncRNAs. However, *PCAT-1* does exhibit a smaller degree of nuclear expression (see Supplementary Figure 12A), which may account for our previous observation that *PCAT-1* may associate with the nuclear Polycomb Repressive Complex 2 (PRC2). As such, while our data directly support a role for *PCAT-1* in the post-transcriptional regulation of *BRCA2*, we cannot fully exclude the possibility of additional regulation of *BRCA2* at the transcriptional level at this time.

In addition, while the mechanism underlying *PCAT-1* function remains incompletely understood, we were intrigued that the 5′ portion of the *PCAT-1* RNA, which is comprised of fully unique sequences, was critical for its regulation of *BRCA2* mRNA whereas the embedded Alu element was not. While we did not identify a specific microRNA with high-confidence 7-mer complementary basepair matching to both this region of *PCAT-1* and *BRCA2* (data not shown), we speculate that alternative mechanisms of miRNA-like mismatch base pairing may contribute to *PCAT-1*-mediated regulation in a manner similar to the recently described networks of competing endogenous RNAs (ceRNAs) (27).

Together, our data suggest that lncRNAs may have a more widespread role in mammalian genome maintenance and DNA repair than previously appreciated. In support of this, a role for small RNAs in human DNA damage repair in human cells has been recently reported and shown to be dependent upon the microRNA biogenesis machinery (28). Of note, Adamson et al. nominated the RNA-binding protein *RBMX* as a novel component of the HR pathway (16), suggesting that RNA-protein interactions may be integral to this process.

This work sheds insight onto potential mechanisms of impaired DSB repair in cancers lacking an inactivating mutation in canonical DSB repair proteins. Thus, our studies have uncovered a novel mechanism of “BRCA-ness”—the clinical observation that many cancers lacking BRCA1/BRCA2 mutations exhibit the clinical features of impaired DSB repair (2, 29, 30). We hypothesize that other cancers with a BRCA-like phenotype may harbor lncRNAs involved in the regulation and execution of proper HR and other forms of DSB repair. Finally, future clinical trials examining the efficacy of PARP1 inhibitors in prostate cancer will provide critical information as to whether *PCAT-1* may serve as a predictive biomarker for patient response to PARP1 inhibitor therapy.

Supplementary Material

Refer to Web version on PubMed Central for supplementary material.

Acknowledgments

We thank Mats Ljungman, Saravana M. Dhanasekaran, Chad Brenner, Yi-Mi Wu, Daniel Robinson, Sameek Roychowdhury, and Dan Hamstra for helpful discussions. We thank Benjamin Chandler for technical assistance. This work was supported in part by the Prostate Cancer Foundation (F.Y.F. and A.M.C.), NIH Prostate Specialized Program of Research Excellence grant P50CA69568, Department of Defense grants PC094231 (F.Y.F.) and PC100171 (A.M.C.), the Early Detection Research Network grant UO1 CA111275 (A.M.C.), the Prostate Cancer Foundation-Movember Challenge Award (to K.E.K., F.Y.F., and M.A.R.), the US National Institutes of Health R01CA132874-01A1 (A.M.C.) and R01CA152057 (M.A.R., F.D.), and the National Center for Functional Genomics support by the Department of Defense (to A.M.C.). A.M.C. is also supported by the Doris Duke Charitable Foundation Clinical Scientist Award and the Howard Hughes Medical Institute. A.M.C. is an American Cancer Society Research Professor and a Taubman Scholar of the University of Michigan. J.R.P., M.K.I, and Q.C. were supported by the Department of Defense Fellowship grants PC094290 (to J.R.P), BC100238 (to M.K.I) and PC094725 (to Q.C.). J.R.P. was supported by a Prostate Cancer Foundation Young Investigator award. J.R.P., A.S., and M.K.I. are Fellows of the University of Michigan Medical Scientist Training Program.

References

1. Negrini S, Gorgoulis VG, Halazonetis TD. Genomic instability--an evolving hallmark of cancer. Nat Rev Mol Cell Biol. 2010; 11:220–8. [PubMed: 20177397]

2. Turner N, Tutt A, Ashworth A. Hallmarks of 'BRCAness' in sporadic cancers. Nat Rev Cancer. 2004; 4:814–9. [PubMed: 15510162]
3. Turner NC, Reis-Filho JS, Russell AM, Springall RJ, Ryder K, Steele D, et al. BRCA1 dysfunction in sporadic basal-like breast cancer. Oncogene. 2007; 26:2126–32. [PubMed: 17016441]
4. Jackson SP, Bartek J. The DNA-damage response in human biology and disease. Nature. 2009; 461:1071–8. [PubMed: 19847258]
5. Roy R, Chun J, Powell SN. BRCA1 and BRCA2: different roles in a common pathway of genome protection. Nat Rev Cancer. 2012; 12:68–78. [PubMed: 22193408]
6. Farmer H, McCabe N, Lord CJ, Tutt AN, Johnson DA, Richardson TB, et al. Targeting the DNA repair defect in BRCA mutant cells as a therapeutic strategy. Nature. 2005; 434:917–21. [PubMed: 15829967]
7. Bryant HE, Schultz N, Thomas HD, Parker KM, Flower D, Lopez E, et al. Specific killing of BRCA2-deficient tumours with inhibitors of poly(ADP-ribose) polymerase. Nature. 2005; 434:913–7. [PubMed: 15829966]
8. Fong PC, Boss DS, Yap TA, Tutt A, Wu P, Mergui-Roelvink M, et al. Inhibition of poly(ADP-ribose) polymerase in tumors from BRCA mutation carriers. N Engl J Med. 2009; 361:123–34. [PubMed: 19553641]
9. Huarte M, Rinn JL. Large non-coding RNAs: missing links in cancer? Hum Mol Genet. 2010; 19:R152–61. [PubMed: 20729297]
10. Prensner JR, Iyer MK, Balbin OA, Dhanasekaran SM, Cao Q, Brenner JC, et al. Transcriptome sequencing across a prostate cancer cohort identifies PCAT-1, an unannotated lincRNA implicated in disease progression. Nat Biotechnol. 2011; 29:742–9. [PubMed: 21804560]
11. Gupta RA, Shah N, Wang KC, Kim J, Horlings HM, Wong DJ, et al. Long non-coding RNA HOTAIR reprograms chromatin state to promote cancer metastasis. Nature. 2010; 464:1071–6. [PubMed: 20393566]
12. Prensner JR, Chinnaiyan AM. The emergence of lncRNAs in cancer biology. Cancer Discov. 2011; 1:391–407. [PubMed: 22096659]
13. Rinn JL, Kertesz M, Wang JK, Squazzo SL, Xu X, Brugmann SA, et al. Functional demarcation of active and silent chromatin domains in human HOX loci by noncoding RNAs. Cell. 2007; 129:1311–23. [PubMed: 17604720]
14. Wan G, Hu X, Liu Y, Han C, Sood AK, Calin GA, et al. A novel non-coding RNA lncRNA-JADE connects DNA damage signalling to histone H4 acetylation. EMBO J. 2013; 32:2833–47. [PubMed: 24097061]
15. Wan G, Mathur R, Hu X, Liu Y, Zhang X, Peng G, et al. Long non-coding RNA ANRIL (CDKN2B-AS) is induced by the ATM-E2F1 signaling pathway. Cell Signal. 2013; 25:1086–95. [PubMed: 23416462]
16. Adamson B, Smogorzewska A, Sigoillot FD, King RW, Elledge SJ. A genome-wide homologous recombination screen identifies the RNA-binding protein RBMX as a component of the DNA-damage response. Nat Cell Biol. 2012; 14:318–28. [PubMed: 22344029]
17. Weinstock DM, Nakanishi K, Helgadottir HR, Jasin M. Assaying double-strand break repair pathway choice in mammalian cells using a targeted endonuclease or the RAG recombinase. Methods Enzymol. 2006; 409:524–40. [PubMed: 16793422]
18. Baumann P, Benson FE, West SC. Human Rad51 protein promotes ATP-dependent homologous pairing and strand transfer reactions in vitro. Cell. 1996; 87:757–66. [PubMed: 8929543]
19. Wahlberg E, Karlberg T, Kouznetsova E, Markova N, Macchiarulo A, Thorsell AG, et al. Family-wide chemical profiling and structural analysis of PARP and tankyrase inhibitors. Nat Biotechnol. 2012; 30:283–8. [PubMed: 22343925]
20. Wang KC, Yang YW, Liu B, Sanyal A, Corces-Zimmerman R, Chen Y, et al. A long noncoding RNA maintains active chromatin to coordinate homeotic gene expression. Nature. 2011; 472:120–4. [PubMed: 21423168]
21. Gong C, Maquat LE. lncRNAs transactivate STAU1-mediated mRNA decay by duplexing with 3′ UTRs via Alu elements. Nature. 2011; 470:284–8. [PubMed: 21307942]
22. Bartel DP. MicroRNAs: target recognition and regulatory functions. Cell. 2009; 136:215–33. [PubMed: 19167326]

23. Tsai MC, Manor O, Wan Y, Mosammaparast N, Wang JK, Lan F, et al. Long noncoding RNA as modular scaffold of histone modification complexes. Science. 2010; 329:689–93. [PubMed: 20616235]
24. Prensner JR, Iyer MK, Sahu A, Asangani IA, Cao Q, Patel L, et al. The long noncoding RNA SChLAP1 promotes aggressive prostate cancer and antagonizes the SWI/SNF complex. Nat Genet. 2013; 45:1392–8. [PubMed: 24076601]
25. Wang D, Garcia-Bassets I, Benner C, Li W, Su X, Zhou Y, et al. Reprogramming transcription by distinct classes of enhancers functionally defined by eRNA. Nature. 2011; 474:390–4. [PubMed: 21572438]
26. Cesana M, Cacchiarelli D, Legnini I, Santini T, Sthandier O, Chinappi M, et al. A long noncoding RNA controls muscle differentiation by functioning as a competing endogenous RNA. Cell. 2011; 147:358–69. [PubMed: 22000014]
27. Salmena L, Poliseno L, Tay Y, Kats L, Pandolfi PP. A ceRNA hypothesis: the Rosetta Stone of a hidden RNA language? Cell. 2011; 146:353–8. [PubMed: 21802130]
28. Francia S, Michelini F, Saxena A, Tang D, de Hoon M, Anelli V, et al. Site-specific DICER and DROSHA RNA products control the DNA-damage response. Nature. 2012; 488:231–5. [PubMed: 22722852]
29. Konstantinopoulos PA, Spentzos D, Karlan BY, Taniguchi T, Fountzilas E, Francoeur N, et al. Gene expression profile of BRCAness that correlates with responsiveness to chemotherapy and with outcome in patients with epithelial ovarian cancer. J Clin Oncol. 2010; 28:3555–61. [PubMed: 20547991]
30. Oonk AM, van Rijn C, Smits MM, Mulder L, Laddach N, Savola SP, et al. Clinical correlates of ‘BRCAness’ in triple-negative breast cancer of patients receiving adjuvant chemotherapy. Ann Oncol. 2012; 23:2301–5. [PubMed: 22357256]

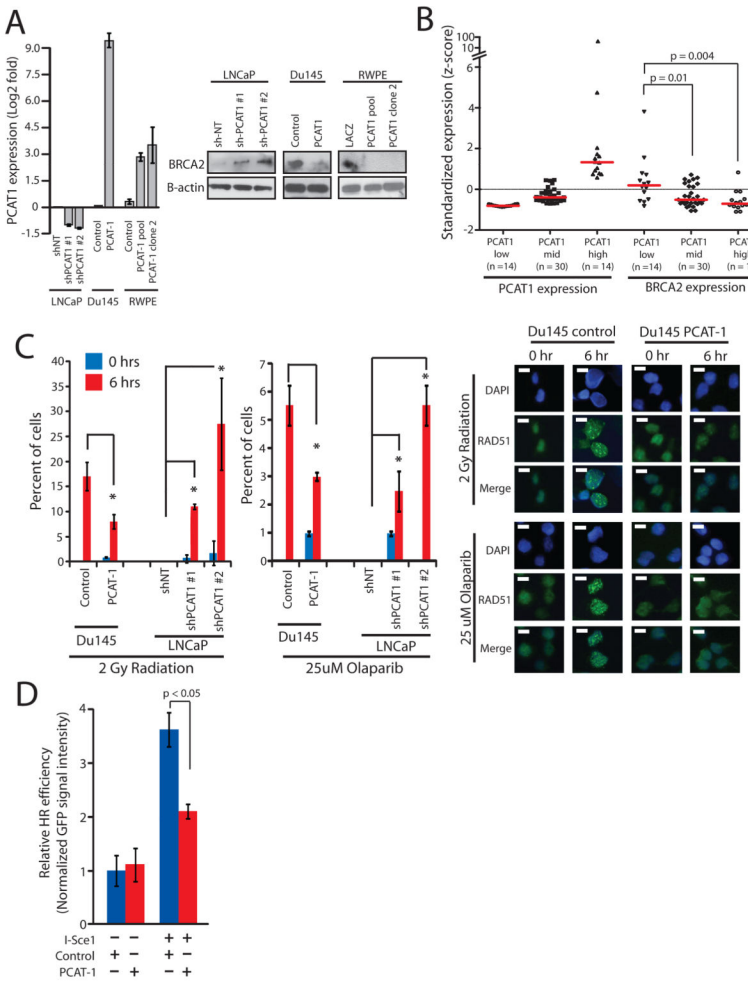

Figure 1.

PCAT-1 expression leads to defective homologous recombination in prostate cells. **A**, *Left*, Expression level of *PCAT-1* by qPCR in three isogenic cell lines with overexpression (Du145, RWPE) or knockdown (LNCaP) of *PCAT-1*. Error bars indicate S.E.M. *Right*, Western blot analysis of BRCA2 in three isogenic cell lines with overexpression (Du145, RWPE) or knockdown (LNCaP) of *PCAT-1*. **B,** Expression of *PCAT-1* and *BRCA2* in a cohort of prostate cancer patients. Expression is shown as z-scores and stratified by increasing *PCAT-1* expression. P values are determined by a Mann-Whitney U test. **C**, *Left*, Quantification of RAD51 foci in isogenic Du145 and LNCaP cell lines following 2 Gy of radiation or treatment with 25uM Olaparib. For LNCaP cell line models, cells with > 5 foci per cell were quantified. For Du145 cell line models, cells with > 10 foci per cell were quantified. Error bars represent standard deviation. An asterisk (*) indicates $p < 0.05$ by Student's t-test. *Right*, Induction of RAD51 foci in Du145-*PCAT-1* cells following 2 Gy of ionizing radiation or treatment with 25uM Olaparib. **D**, I-SceI-mediated GFP HR assay in PC3-*PCAT-1* cells compared to matched control cells. Error bars represent S.E.M.

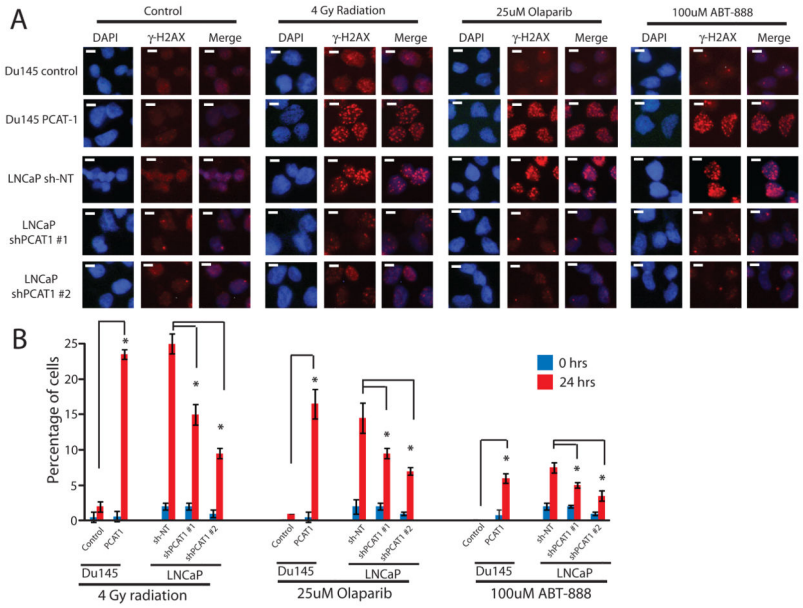

Figure 2.

PCAT-1 knockdown reduces γH2AX foci formation following genotoxic stress. **A**, LNCaP or Du145 cells with knockdown or overexpression for *PCAT-1* were subjected to 4 Gy of ionizing radiation, 25uM Olaparib, 100uM of ABT-888, or control DMSO. 24 hours post-treatment, cells were fixed and stained for γH2AX and counterstained for DAPI. **B**, Quantification of γH2AX foci in LNCaP and Du145 isogenic *PCAT-1* cells treated with radiation or PARP inhibitors. For LNCaP cell line models, cells with > 5 foci per cell were quantified. For Du145 cell line models, cells with > 10 foci per cell were quantified. Error bars represent the standard deviation. An asterisk (*) indicates $p < 0.05$ by Student's t-test.

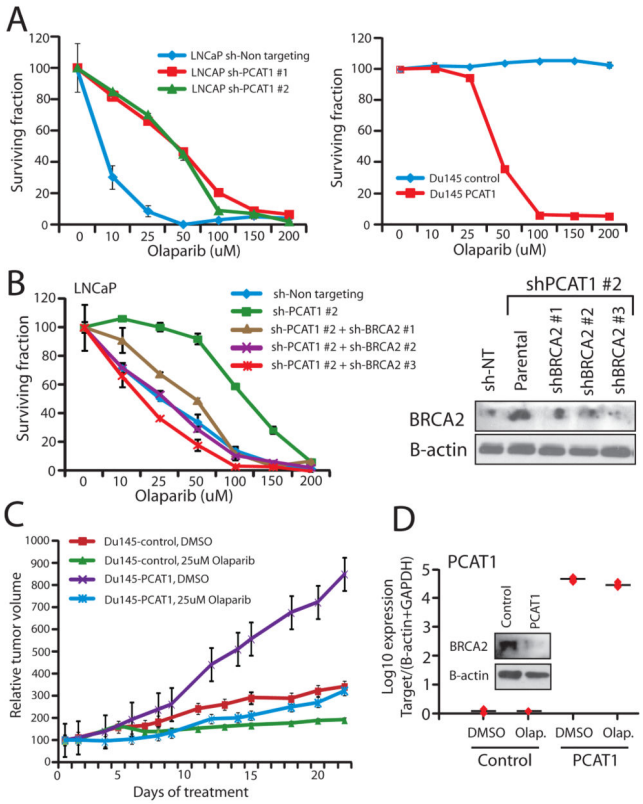

Figure 3.

PCAT-1 expression results in prostate cell sensitivity to PARP inhibition *in vitro* and *in vivo*. **A**, *Left*, LNCaP cells with *PCAT-1* knockdown exhibit enhanced cell survival 72 hrs post-treatment with Olaparib. *Right*, Du145 cells with *PCAT-1* overexpression exhibit reduced cell survival 72 hrs post-treatment with Olaparib. Cell survival is determined via WST assays. **B**, *BRCA2* knockdown in LNCaP sh*PCAT-1* cells rescues cell sensitivity to Olaparib. An inset Western blot showing efficiency of BRCA2 knockdown is included. **C**, Tumor growth curves for Du145-control and Du145-*PCAT-1* xenografts following initiation of treatment with DMSO control or 25uM Olaparib. Tumor volumes are normalized to 100, and time = 0 represents the start of treatment administration. Treatment was initiated three weeks after xenograft engraftment. **D**, Expression level of *PCAT-1*and BRCA2 protein in Du145-*PCAT-1* xenografts. Error bars in this figure represent +/− S.E.M.

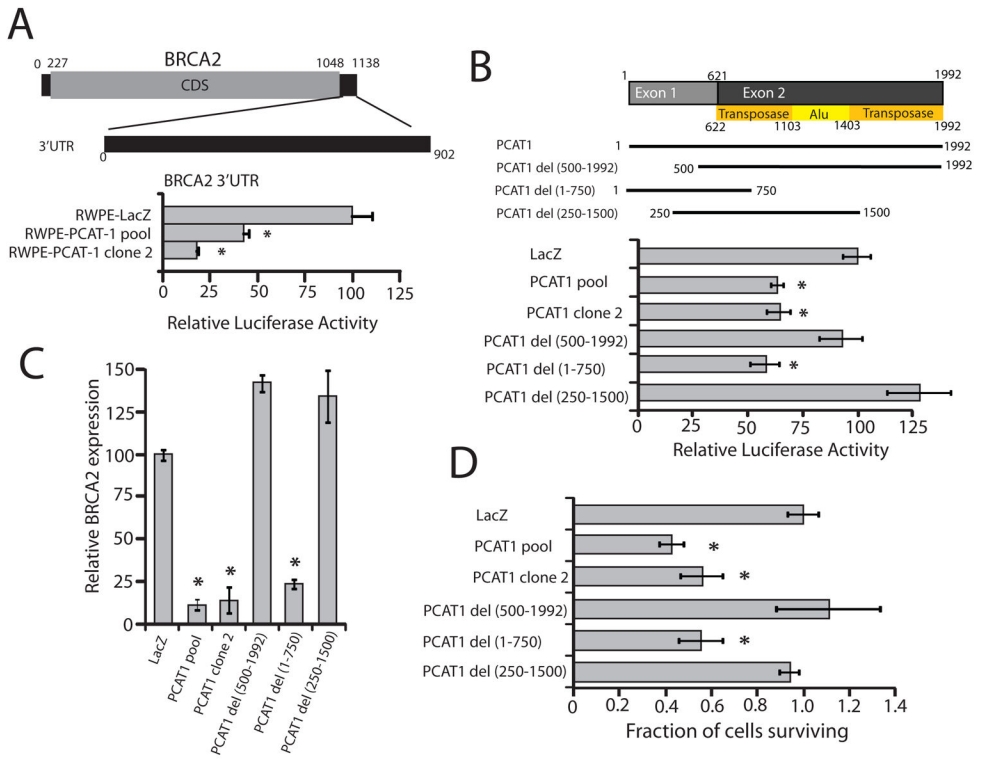

Figure 4.

The 5′ terminus of *PCAT-1* represses *BRCA2* mRNA via the 3′UTR of *BRCA2*. **A**, Transfection of a *BRCA2* 3′UTR luciferase construct in RWPE-*PCAT-1* cells. **B**, A schematic of *PCAT-1* deletion constructs overexpressed in RWPE cells. *PCAT-1* del (1-750 bps) was able to recapitulate repression of the *BRCA2* 3′UTR luciferase construct. **C**, Endogenous *BRCA2* transcript levels in RWPE cells overexpressing *PCAT-1* deletion constructs. **D**, Treatment of RWPE cells overexpressing *PCAT-1* deletion constructs with 25uM Olaparib. Cell survival was measured 72 hrs post-treatment with WST. Error bars in this figure represent +/− S.E.M. An asterisk (*) indicates $p < 0.05$ by Student's t-test.